Check for updates

ECOLOGY

Elevated CO_2 mitigated warming-enhanced carbon loss from northern peatland

Jian Zhou[1], Quan Quan[1], Wenjuan Huang[2], Paul J. Hanson[3], Daniel Ricciuto[3], Melanie A. Mayes[3], Natalie A. Griffiths[3], Verity G. Salmon[3], Sören Eliot Weber[3,4], Jeffrey M. Warren[3], Richard J. Norby[3,5], Mara Y. McPartland[6], Mirindi Eric Dusenge[7], Danielle Way[7,8,9], Lifen Jiang[1], Yu Zhou[10], Haodi Xu[1], Feng Tao[11,12], Xiaoying Shi[3], Weinan Chen[1], Yahai Zhang[1], Yiqi Luo[1]*

Copyright © 2026 The Authors, some rights reserved; exclusive licensee American Association for the Advancement of Science. No claim to original U.S. Government Works. Distributed under a Creative Commons Attribution NonCommercial License 4.0 (CC BY-NC).

Peatlands store one-third of the global soil carbon (C) on only ~3% of Earth's land surface but risk becoming C sources to accelerate climate change due to warming-induced C loss. Elevated CO_2 (eCO_2) may mitigate this loss by boosting plant C uptake. However, how eCO_2 and climate warming interact to influence peatland C dynamics remains unclear. Here, we investigated peatland C fate at five warming levels (+0°, +2.25°, +4.5°, +6.75°, and + 9°C), each under ambient CO_2 (aCO_2) and eCO_2 (+500 parts per million), by model-guided synthesis of 18 measured variables for each of the 10 treatments from an experiment. Our results showed that the peatland C loss increased with warming at a rate of 62.6 g C m^{-2} $year^{-1}$°C^{-1}, reaching 476.5 ± 104.7 g C m^{-2} $year^{-1}$ at +9°C under aCO_2, primarily because of increased *Sphagnum* mortality and accelerated decomposition. eCO_2 reduced the loss rate to 17.3 g C m^{-2} $year^{-1}$°C^{-1}, nearly halving the C loss at +9°C (269.4 ± 80.5 g C m^{-2} $year^{-1}$), mainly due to enhanced tree and shrub growth. Methane emissions increased with warming, similarly under aCO_2 and eCO_2. Our findings suggest that northern peatlands likely become major C sources under climate warming, although rising atmospheric CO_2 concentration may partially slow down the C loss. Climate-driven shifts in plant community structure, rather than peat decomposition alone, play a critical role in regulating peatland C fate and may threaten the stability of peatland ecosystem functions and services in the future.

INTRODUCTION

Peatlands serve as a long-term carbon (C) sink that contributes to global climate cooling (*1*–*3*), and disproportionately store a substantial volume of C-rich peat (*4*, *5*). Northern peatland C has been protected by low temperatures and anaerobic environments (*6*) over millennia. By the end of this century, temperatures in high-latitude regions, where the vast majority of peatlands are located, are predicted to rise by up to 8.3°C under extreme climate change scenarios (*7*, *8*), which could trigger massive C loss, risking peatlands becoming C sources (*9*–*12*). However, the vulnerability of peatland C to warming may be lessened by a concomitant increase in atmospheric CO_2 concentration (eCO_2) that can enhance plant C uptake and may increase soil organic carbon (SOC) stocks (*13*). Nonetheless, the extent to which eCO_2 interacts with warming to influence net peatland C balance remains unclear, leading to variable predictions about the future role of peatlands in the global C cycle, ranging from a sustained C sink (*2*) to a major C source (*11*, *14*). This uncertainty underscores a critical knowledge gap in our understanding of peatland responses to climate warming and eCO_2 and their underlying mechanisms.

Climate warming and eCO_2 can trigger a myriad of process changes to influence peatland C dynamics. A 3-year synthesis of observations from a peatland experiment manipulating warming and eCO_2 showed rapid warming-induced C loss with negligible effects of eCO_2, primarily due to enhanced peat decomposition (*11*). Consistent with this observation, most previous studies that project the future fate of peatland C are focused on peat decomposition in response to warming (*4*, *10*, *15*). However, over longer timescales, temperature acclimation and adaptation can reduce the sensitivity of C loss to warming (*16*, *17*), resulting in lower C emissions than predictions assuming constant temperature sensitivity (*18*). Whether these longer-term responses reduce the relative importance of peat decomposition in peatland C balance remains uncertain, as warming may continue to increase the vulnerability of large peat C stocks accumulated under historically cold and waterlogged conditions. This leads to our first hypothesis that warming stimulates C loss primarily through accelerated peat decomposition under ambient CO_2 (aCO_2). On the other hand, the responses of plant C uptake in peatlands to global change have received less attention than peat decomposition in peatland research. Although the CO_2 fertilization effect that is frequently observed on leaf photosynthesis may be dampened due to limited nutrient availability (*19*, *20*), especially in nutrient-poor ombrotrophic bogs, the CO_2 fertilization effect may be amplified over longer timescales if eCO_2 leads to leaf area increases (*21*) and/or plant community structure changes (*22*). Furthermore, although multifactorial experiments have primarily indicated additive effects of global change factors (*23*), interactions between eCO_2 and warming are often observed due to altered plant composition and other physiological processes (*24*, *25*). These changes could enhance plant C uptake and offset warming-induced C losses through

[1]Soil and Crop Sciences Section, School of Integrative Plant Science, Cornell University, Ithaca, NY, USA. [2]Department of Ecology, Evolution, and Organismal Biology, Iowa State University, Ames, IA, USA. [3]Environmental Sciences Division, Oak Ridge National Laboratory, Oak Ridge, TN, USA. [4]Department of Biology, West Virginia University, Morgantown, WV, USA. [5]Ecology and Evolutionary Biology, University of Tennessee, Knoxville, TN, USA. [6]Institue for Earth System Science & Remote Sensing, Leipzig University, Leipzig, Germany. [7]Division of Plant Science, Research School of Biology, The Australian National University, Canberra, Australia. [8]Department of Biology, The University of Western Ontario, London, ON, Canada. [9]Nicholas School of the Environment, Duke University, Durham, NC, USA. [10]Department of Environmental Systems Science, ETH Zurich, Zurich, Switzerland. [11]College of Information Sciences and Technology, Pennsylvania State University, University Park, PA, USA. [12]Institute of Energy and the Environment, Pennsylvania State University, University Park, PA, USA.
*Corresponding author. Email: yl2735@cornell.edu

Downloaded from https://www.science.org at Cornell University on October 30, 2026

peat decomposition. We therefore postulate a second hypothesis that elevated CO_2 mitigates peatland C loss through its interactive effects with climate warming.

We tested the above hypotheses using data from the Spruce and Peatland Responses Under Changing Environments (SPRUCE) experiment, a large-scale, two-factor experiment conducted in an ombrotrophic bog, in northern Minnesota (United States), with five warming levels (+0°, +2.25°, +4.5°, +6.75°, and + 9°C; belowground since 2014 and aboveground since 2015), each under two CO_2 treatment levels [ambient and +500 parts per million (ppm); since 2016] (see Materials and Methods) (*11*, *26*, *27*). While the previous synthesis of observations over 3 years at SPRUCE provided important early evidence of peatland C dynamics under warming and CO_2, it primarily relied on empirical functions to upscale monthly CO_2 and CH_4 fluxes measured from large collars into annual estimates and excluded tree photosynthesis or aboveground autotrophic respiration (Ra) (*11*). To more comprehensively examine the longer-term fate of peatland C under warming and eCO_2, we adopted a model-guided data synthesis approach, as used in previous studies to upscale sparse and multiple data sets to estimate ecosystem C balances (*28*, *29*). Specifically, we estimated the annual C budget for each of the 10 treatments by synthesizing 18 observed variables from 2011 to 2021 (table S1) with a process-based modeling framework [Terrestrial ECOsystem (TECO)–SPRUCE] (fig. S1) (*30*, *31*). Estimates from this approach closely match all measured variables (figs. S2 and S3), allowing us to infer peatland C fate under warming and elevated CO_2.

RESULTS

Changes in C fluxes under warming and elevated CO_2

Under aCO_2, warming linearly increased C loss [i.e., net carbon exchange (NCE); note that all the fluxes in this paper have been corrected with pretreatment values to account for baseline variability] at a rate of 62.6 g C m^{-2} $year^{-1}$°C^{-1} across the five warming levels, shifting the ecosystem from a slight C sink of 79.1 ± 61.5 g C m^{-2} $year^{-1}$ at +0°C to a significant C source of 476.5 ± 104.7 g C m^{-2} $year^{-1}$ at +9°C (Fig. 1A). The warming-induced increases in C loss under aCO_2 resulted from both decreasing plant C uptake [i.e., gross primary productivity (GPP); Fig. 1B] and increasing soil C decomposition via both heterotrophic respiration of CO_2 (Rh_{CO_2}) and CH_4 emissions (Fig. 1, E and F), with declining GPP contributing most to the overall C loss (fig. S4). Conversely, eCO_2 reduced the warming-induced C loss rate to 17.3 g C m^{-2} $year^{-1}$°C^{-1}, decreasing C loss by 52.7 and 43.5% (i.e., 212.8 ± 89.3 and 207.1 ± 45 g C m^{-2} $year^{-1}$°C^{-1}) at +6.75° and + 9°C, respectively (Fig. 1A), primarily due to increased plant C uptake (Fig. 1B). The lower NCE at eCO_2 than aCO_2 at +0°C and + 4.5°C (Fig. 1A) was mainly due to decreased net plant C uptake [i.e., net primary productivity (NPP)] and increased Rh_{CO_2} (Fig. 1, C and E).

GPP decreased with temperature under aCO_2 at a rate of 63.5 g C m^{-2} $year^{-1}$°C^{-1}, reaching a reduction of 241.4 ± 111 g C m^{-2} $year^{-1}$ at +9°C (Fig. 1B). eCO_2 mitigated the warming-induced decreases in GPP under high warming treatments (+6.75° and + 9°C) (Fig. 1B), mainly due to eCO_2-driven increases in tree GPP (fig. S5A). NPP declined significantly with temperature under aCO_2 but showed no significant response to warming under eCO_2 (Fig. 1C). Negative eCO_2

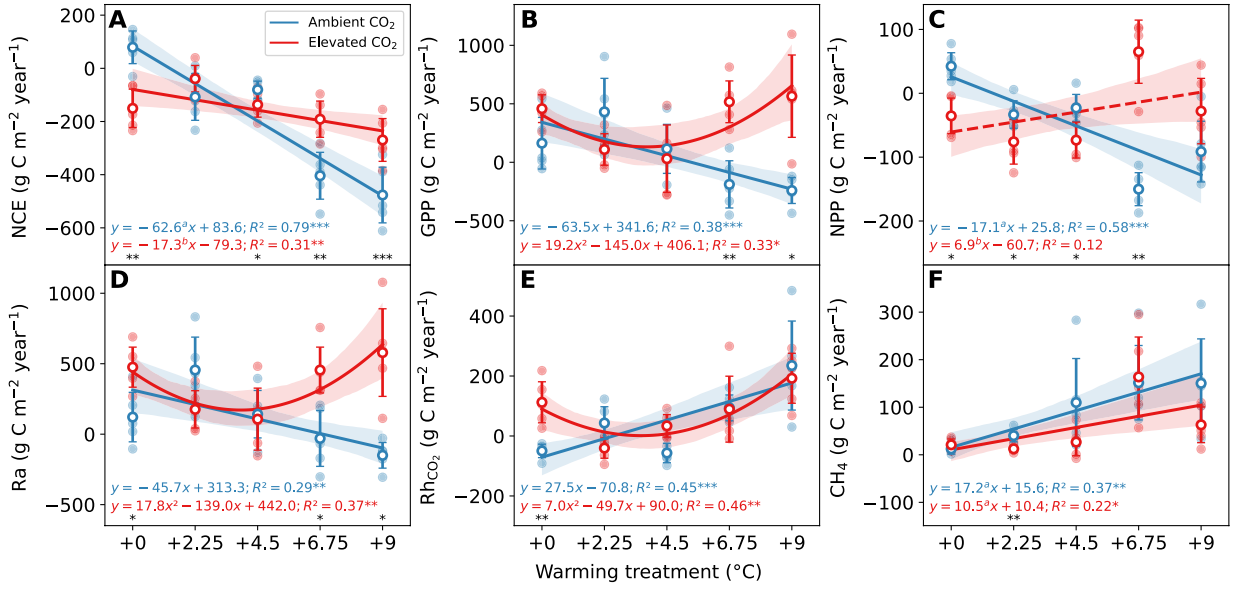


Fig. 1. Changes in C fluxes estimated by the model-guided data synthesis approach at five warming treatment levels under ambient and elevated CO_2 in the peatland. (**A**) NCE. (**B**) GPP. (**C**) NPP. (**D**) Ra. (**E**) Rh_{CO_2}. (**F**) Methane emissions (CH_4). All estimated fluxes were corrected for differences between the treatment years (2017–2021) and the pre-treatment year (2013). Solid dots denote annual values with open dots and error bars indicating mean and SD across years, respectively. The blue and red colors represent data under ambient and elevated CO_2, respectively. The lines and statistics shown are regression results, with solid and dashed lines indicating statistically significant and non-significant relationships, respectively. Different letters (i.e., *a* and *b*) in each equation indicate statistically significant differences (analysis of covariance; $P < 0.05$). The shaded areas represent the 95% confidence intervals. Asterisks above the *x* axis denote significant differences between ambient and elevated CO_2 (paired *t* test) for a given temperature treatment or a significant regression relationship in the equations (*$P < 0.05$, **$P < 0.01$, and ***$P < 0.001$). R^2, coefficient of determination.

Downloaded from https://www.science.org at Cornell University on October 30, 2026

effects on NPP at the warming treatments below +4.5°C (Fig. 1C) were mainly due to eCO_2-induced depression in *Sphagnum* growth, potentially driven by increased shading effect (*32*) and consistent with similar suppressive eCO_2 effects reported in other studies (*33*, *34*). At +6.75°C, NPP was much higher under eCO_2 than aCO_2, which was associated with substantial stimulation of GPP by eCO_2 despite an increase in Ra (Fig. 1D).

Heterotrophic CO_2 emissions increased linearly with warming at 27.5 g C m^{-2} $year^{-1}$°C^{-1} under aCO_2, reaching 234.9 ± 148.5 g C m^{-2} $year^{-1}$ at +9°C (Fig. 1E). Although CO_2 emissions changed nonlinearly with warming under eCO_2, the differences in CO_2 emissions between aCO_2 and eCO_2 were not significant under each warming level, except at +0°C. This suggests that eCO_2-driven priming in our study was not as substantial as in other studies that found extra plant C inputs under eCO_2 fuel soil C decomposition via priming for mining additional nutrients (*35*, *36*). At this site, warming-induced mortality of *Sphagnum* mosses may have supplied extra nutrients for eCO_2-stimulated plant growth (*37*). CH_4 emissions increased linearly with warming under both aCO_2 and eCO_2 (Fig. 1F), probably through thermodynamic stimulation and increased substrate availability (*10*, *15*). While mean annual water-table depth did not significantly change among the 10 experimental plots over the treatment period (2017–2021) [fig. S6; except during the extreme drought event in 2021 (*38*)], heterotrophic CO_2 emissions were significantly correlated with water-table depth under aCO_2 (fig. S7), consistent with previous findings (*39*).

Changes in C pools under warming and elevated CO_2

Substantial changes in C fluxes under warming and eCO_2 treatments were reflected in changes in C storage in different pools (Fig. 2). The annual change in plant C storage showed no significant responses to warming under aCO_2 but increased with warming under eCO_2 (Fig. 2A), partially due to increased GPP in response to warming (Fig. 1B). The annual change in litter C pool significantly decreased with warming under both aCO_2 and eCO_2 (Fig. 2B). Warming stimulated substantial soil C losses under aCO_2 via enhanced decomposition and reduced C input from *Sphagnum*, while eCO_2 mitigated warming-induced soil C losses mainly through increased C input from tree and shrub growth (Figs. 2C and 3). This is consistent with a previous study that warming alone increased peatland SOC loss whereas the combination of warming and eCO_2 partially alleviated the warming-induced SOC loss by increasing plant-derived C inputs (*40*). The interactive effects of warming and eCO_2 resulted in less decreases in total ecosystem C storage at +4.5° and + 9°C under eCO_2 than aCO_2 (Fig. 2D).

Differential responses of PFTs to eCO_2 under warming

To quantify alleviation of ecosystem C loss by eCO_2, we calculated differences in C fluxes between eCO_2 and aCO_2 at each of the warming levels. The effect of eCO_2 on NCE exhibited a linear response to warming (Fig. 3A), primarily due to the eCO_2 stimulation of tree and shrub NPP (Fig. 3B). Tree NPP showed no response to warming under aCO_2 but increased under eCO_2 (Fig. 3C), with a significant eCO_2-induced enhancement at +2.25°, +6.75°, and + 9°C. Shrub

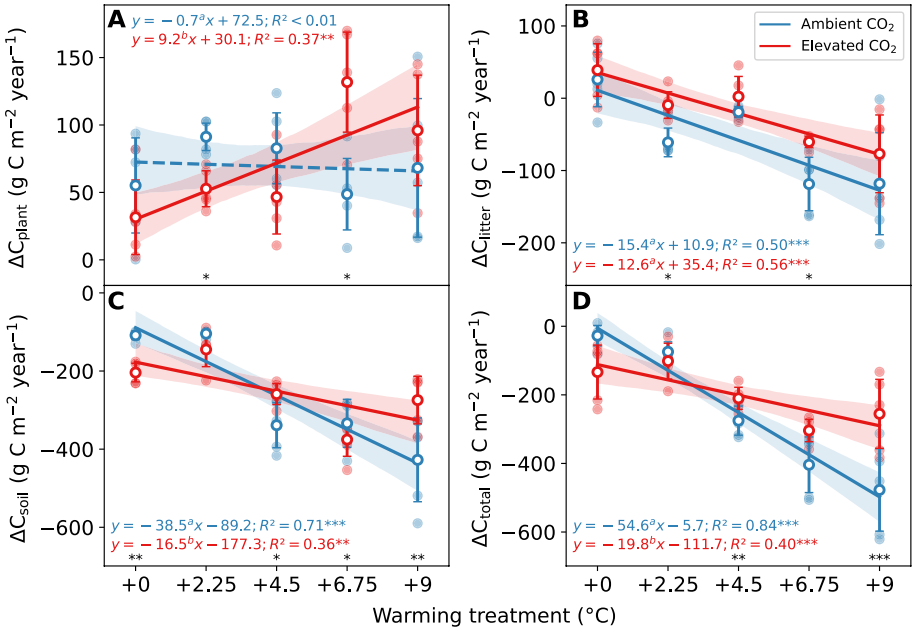


Fig. 2. Annual changes in C pools in the peatland at five warming treatment levels under ambient and elevated CO_2. The change in the size of the annual C pool was calculated as the difference between the C stock of the current year and that of the previous year for total plant C pool (ΔC_{plant}) (**A**), litter C pool (ΔC_{litter}) (**B**), soil C pool (ΔC_{soil}) (**C**), and total ecosystem C pool (ΔC_{total}) (**D**). The open dots and error bars indicate mean and SD of estimates from multiple years (2017–2021) derived using the model-guided data synthesis approach, respectively, and solid dots denote yearly values. The blue and red colors represent data under ambient and elevated CO_2, respectively. The lines and statistics shown are regression results, with solid and dashed lines indicating statistically significant and non-significant relationships, respectively. The shaded areas represent the 95% confidence intervals. Different letters (i.e., *a* and *b*) in each equation indicate statistical significance (analysis of covariance; $P < 0.05$). Asterisks above the *x* axis denote a significant CO_2 effect (paired *t* test), and those within the equations indicate significant regression relationships (*$P < 0.05$* **$P < 0.01$, and ***$P < 0.001$).

Downloaded from https://www.science.org at Cornell University on October 30, 2026

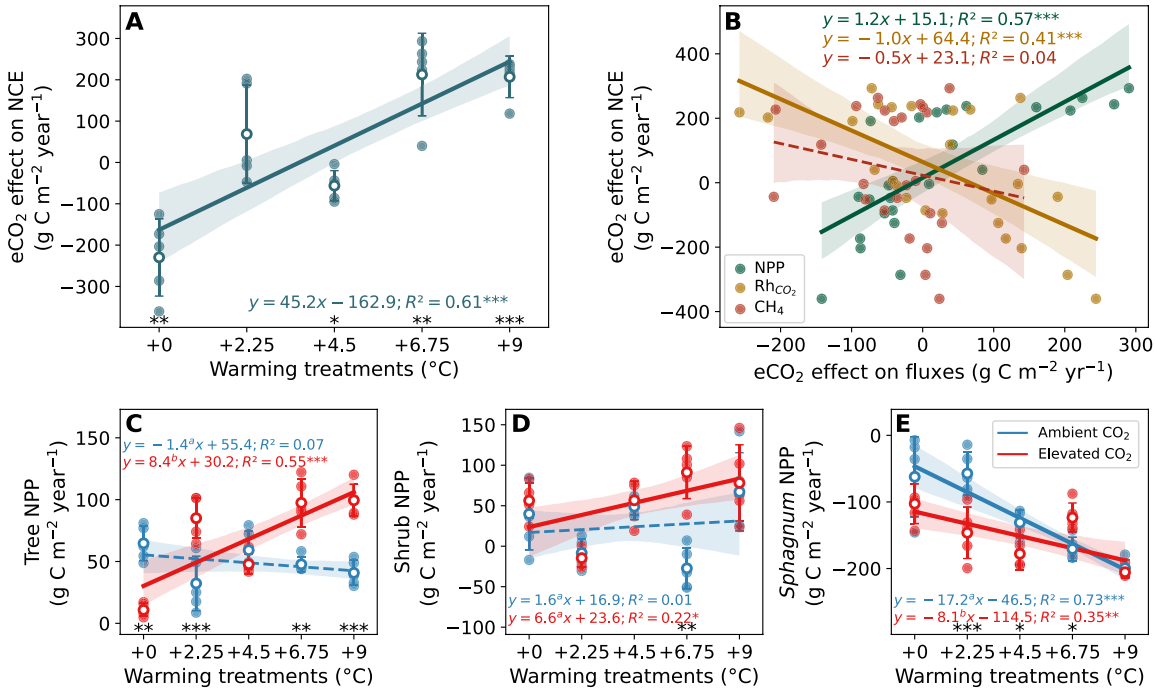


Fig. 3. Elevated CO_2 (eCO_2) effect on NCE and its components across warming treatments. (**A**) eCO_2 effect on NCE at different warming treatment levels. (**B**) Relationships between the eCO_2 effect on NCE and the eCO_2 effect on flux components: NPP, Rh_{CO_2}, and methane emissions (CH_4). (**C** to **E**) Tree, shrub, and *Sphagnum* NPP across warming levels, respectively. Solid dots denote annual values estimated by the model-guided data synthesis approach from 2017 to 2021 with open dots and error bars indicating mean and SD across years, respectively. All estimated fluxes were corrected for differences between the treatment years (2017–2021) and the pretreatment year (2013). The lines and statistics shown are regression results, with solid and dashed lines indicating statistically significant and nonsignificant relationships, respectively. Shaded areas show 95% confidence intervals. Different letters (e.g., *a*, *b*, and *c*) in each equation indicate statistical significance (analysis of covariance; $P < 0.05$). Asterisks above the *x* axis denote a significant CO_2 effect (paired *t* test), and those within the equations indicate significant regression relationships (*$P < 0.05$, **$P < 0.01$, and ***$P < 0.001$).

NPP exhibited the same trend as tree NPP (Fig. 3D and fig. S8B), supported by previously reported increases in shrub photosynthetic rate under eCO_2 (*41*) and leaf area index (LAI) with warming (*42*). *Sphagnum* productivity declined with warming under both aCO_2 and eCO_2 (Fig. 3E and fig. S8, C and D), driven by warming/desiccation-induced mortality (*43*) and shading by trees and shrubs (*32*). While differential changes in growth of the three plant functional types (PFTs) (i.e., trees, shrubs, and *Sphagnum*) significantly altered the annual C balance, their long-term impacts will depend on changes in litter quality and composition, which can have cascading effects on peat decomposition (*40*, *44*).

Contributions of ecosystem property changes to the eCO_2 effect on C fluxes under warming

We assessed the importance of altered plant community structure and other ecosystem properties (e.g., temperature sensitivity of CH_4 production), as reflected in varying parameters (fig. S9), in regulating the ecosystem-scale C balance through a modeling experiment. Specifically, estimated parameters at the control plot (i.e., +0°C and aCO_2) from 2011 to 2013 (before the experimental treatments) were used in TECO-SPRUCE for simulating peatland responses to the five warming treatments each under aCO_2 and eCO_2 levels from 2014 to 2021 (see Materials and Methods). This experiment mimicked conventional simulation modeling with fixed parameter values, assuming no changes in ecosystem properties under climate change (*45*), compared with using varying parameters to capture these ecosystem property changes (as done in this study). The latter approach was conceptually similar to trait-based modeling via adjusting parameter values with traits (*46*, *47*). Without ecosystem property changes, most C fluxes showed significant responses to warming and eCO_2 (fig. S10) in sharp contrast with the patterns estimated by the data-informed model (Fig. 1). The contribution of ecosystem property changes to the eCO_2 effect on NCE linearly rose with warming at a rate of 35.3 g C m^{-2} $year^{-1}$°C^{-1} (Fig. 4A). This increased NCE was primarily attributed to changes in NPP (Fig. 4B), resulting from differential responses of the three PFTs to warming and eCO_2 with and without ecosystem property changes (Fig. 4C). Overall, ecosystem property changes reduced the estimated eCO_2 effect on NPP and heterotrophic respiration compared with the model using fixed parameters (Fig. 4C), consistent with widely reported ecosystem acclimation to climate change (*48*, *49*).

DISCUSSION

Our findings deepen the mechanistic understanding of peatland C cycling in response to warming and eCO_2. While most studies have focused on peat decomposition and its response to warming for predicting peatland future C dynamics (*10*, *15*, *50*, *51*), we highlight the pivotal role of ecosystem property changes (i.e., changes in plant community structure or other ecophysiological properties) in shaping the future C fate of peatlands under climate warming and rising atmospheric CO_2 concentration.

Downloaded from https://www.science.org at Cornell University on October 30, 2026

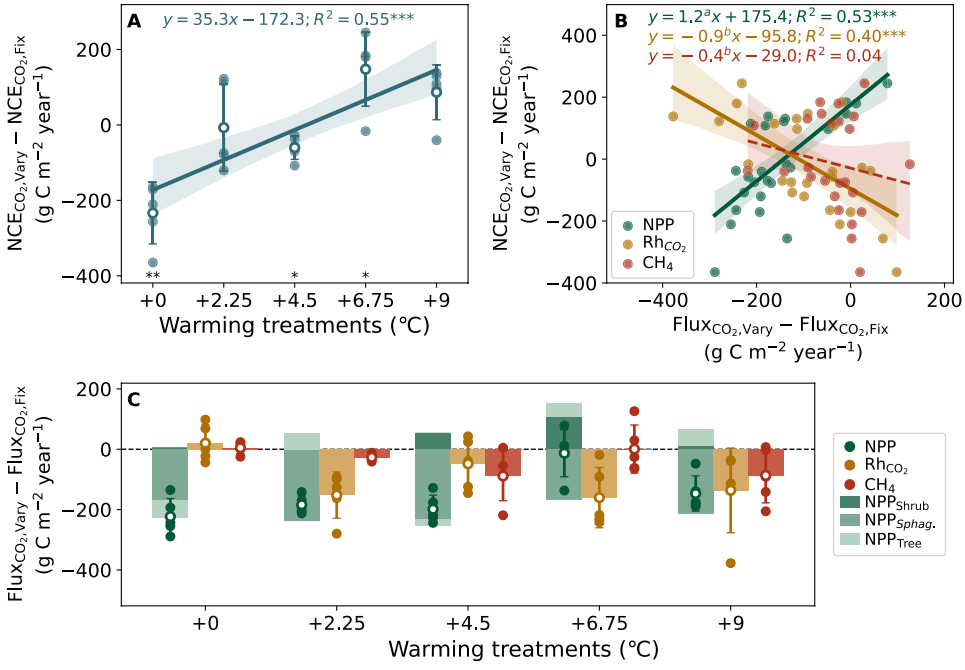


Fig. 4. Effects of ecosystem property changes on eCO_2-induced changes in NCE and its components across warming treatment levels. (**A**) CO_2 effect on NCE with and without ecosystem property changes as calculated by the difference between the CO_2 effect on NCE with varying and fixed parameters ($NCE_{CO2,Vary} - NCE_{CO2,Fix}$). (**B**) Relationships between CO_2 effects on NCE and its flux components with or without ecosystem property changes ($Flux_{CO2,Vary} - Flux_{CO2,Fix}$), including NPP, Rh_{CO_2}, and methane emissions (CH_4). (**C**) Differences in the CO_2 effect on NPP and its three different PFTs (Shrub, *Sphagnum*, and Tree), Rh_{CO_2}, and CH_4 with and without ecosystem property changes. All estimated fluxes were corrected for differences between the treatment years (2017–2021) and the pretreatment year (2013). Fluxes without ecosystem property changes were estimated using fixed parameters from the control experimental plot (+0°C and ambient CO_2) during the pretreatment period (2011–2013). Solid dots denote annual values estimated by the model-guided data synthesis approach with open dots and error bars indicating mean and SD across years, respectively. The lines and statistics shown are regression results, with the solid and dashed line indicating statistically significant and nonsignificant relationships, respectively. Shaded areas show 95% confidence intervals. Asterisks denote significant impacts of ecosystem property changes on eCO_2 effects or significant relationships (*$P < 0.05$, **$P < 0.01$, and ***$P < 0.001$).

Under aCO_2, the warming-induced decrease in plant C uptake, primarily due to increased *Sphagnum* mortality, was the major contributor to NCE declines (fig. S4), thereby partially falsifying the first hypothesis that warming stimulates C loss mainly through accelerated peat decomposition. Although warming-induced decline in *Sphagnum* productivity and enhanced peat decomposition have each been documented previously (*11*, *43*), their relative importance in regulating ecosystem-scale C balance under long-term warming has rarely been quantified within a unified framework. By comprehensively assessing C fate at the whole-ecosystem level, we directly quantified the relative contributions of vegetation-driven C inputs and decomposition-driven C losses to peatland C balance under warming. Our analysis demonstrates that changes in vegetation C uptake play an important yet often underappreciated role, alongside peat decomposition, in determining peatland C balance. This finding broadens current perspectives on peatland C vulnerability to climate change by showing that future ecosystem C balance depends not only on the stability of existing C stocks but also on the capacity of plant communities to sustain C inputs under warming.

Previous experimental studies mostly reported minor interactive effects of warming and eCO_2 on ecosystem C cycling (*11*, *37*, *52*, *53*). However, we found that elevated CO_2 effects increased with warming (i.e., interactive effects) to mitigate warming-induced peatland C loss (Fig. 3A) mainly through differential responses of the three PFTs (Fig. 3, C to E), supporting the second hypothesis. Specifically, eCO_2 promoted shrub and tree growth across five warming levels while suppressing *Sphagnum* growth at moderate warming (Fig. 3, C to E). Previous studies suggest that warming and eCO_2 can favor vascular plant expansion, leading to greater shading of *Sphagnum* and consequently reducing its growth and photosynthetic capacity (*32*). These differential responses among PFTs underpinned the interaction between warming and eCO_2, as enhanced shrub and tree productivity compensated for declines in *Sphagnum* productivity and partially offset C losses from peat decomposition at the ecosystem scale. This result highlights the importance of plant community change in shaping ecosystem responses to warming and eCO_2. Our results are consistent with previous findings that indirect effects of warming and eCO_2 through changes in vegetation structure and other processes are often more important than their direct effects (*21*, *22*, *54*, *55*). Moreover, this study also suggests that climate change–induced shifts in boreal peatland plant community structure may further suppress peat-forming *Sphagnum* mosses, potentially contributing to transitions toward shrub- and tree-dominated ecosystem and reducing critical peatland ecosystem services.

Increasing evidence suggests that climate-driven changes in ecosystem properties can substantially affect ecosystem C cycling (*22*, *49*, *56*). However, these changes are often poorly represented by models using a fixed parameter set but can be captured through varying parameters across different environmental conditions (*18*, *45*). In this study, we represented changes in ecosystem properties related to

Downloaded from https://www.science.org at Cornell University on October 30, 2026

plant community structure and other ecophysiological properties by treatment-specific parameterization. Our results showed that the responses of peatland C balance to warming and eCO_2 were primarily regulated by changes in plant community structure (Fig. 3). We further evaluated the contribution of ecosystem property changes to peatland C dynamics under warming and eCO_2 in a modeling experiment with varied (changed ecosystem properties) versus fixed parameters (unchanged ecosystem properties). Our finding underscores the importance of plant community structure in determining peatland C balance under climate change (Fig. 4). These results also highlight the limitations of current models relying on fixed parameter values to project future peatland C dynamics under climate change. Allowing parameters associated with changing ecophysiological properties to vary across environmental conditions practically represents these changes in ecosystem properties. Nevertheless, it is highly desirable to move beyond parameter-based representation of ecosystem property changes and develop functional relationships of the property changes with environmental drivers to be incorporated for model projection of long-term peatland C dynamics under changing climate.

Water-table dynamics play an important role in regulating peatland C cycling (*39*). However, water-table depth showed no significant changes with warming at either the annual or growing-season scale during the treatment period, except during the extreme drought in 2021 (fig. S6) (*38*). Overall, water-table drawdown during growing season had limited effects on ecosystem-level C fluxes, except for a significant increase in heterotrophic CO_2 respiration (fig. S7, A to F). For individual PFTs, water-table drawdown during the growing-season increased tree productivity but reduced *Sphagnum* productivity under eCO_2 (fig. S7, G and I), consistent with previous evidence that lower water tables can favor woody vegetation while suppressing *Sphagnum* in peatlands (*43*, *57*–*59*). Although the warming treatment did not significantly lower either annual or growing-season mean water-table depth in our study, warming-induced hydrological stress may still be an important driver of *Sphagnum* decline (*43*). Notably, the extreme drought in 2021 caused pronounced water-table drawdown and amplified warming-induced C loss, even more so under eCO_2 (*38*). Therefore, understanding the influence of hydrological change on peatland C dynamics requires consideration of both chronic water-table changes and episodic extreme events, supported by dedicated manipulation experiments and long-term observations.

In addition to the lack of water-table manipulation discussed above, a few additional limitations should be considered in interpreting our results. First, experimental limitations of the SPRUCE experiment, such as uniform and year-round warming, and limited CO_2 treatments to the growing seasons and daytime may not reflect real-world patterns of global change (*9*, *60*, *61*), requiring cautions in interpreting experimental results and extrapolating to larger spatial and temporal scales. Second, our model-guided data synthesis approach integrated and upscaled multiple observations within a process-based framework, effectively capturing treatment-induced ecosystem C dynamics through observation-constrained parameter variation. However, the underlying mechanisms are represented implicitly through parameterization rather than explicitly in model structure. Parameterization may be context dependent, and additional validations would be needed when applied to ecosystems beyond the spatiotemporal domains of the SPRUCE experiment. Third, our findings characterize peatland C dynamics over an 8-year experimental period and reveal that elevated CO_2 buffered warming-induced C loss by stimulating the growth of trees and shrubs. Although the observed interactive effect of warming and elevated CO_2 on peatland C balance was more pronounced than that reported in the previous shorter-term study (*11*), whether this response persists over longer timescales remains uncertain, as plant responses to elevated CO_2 may diminish with stand age (*29*), nutrient limitation (*19*, *62*), and longer-term physiological acclimation (*63*). Moreover, increased plant-derived C inputs may alter the partitioning of C among peat C pools, shifting a greater proportion of C toward faster turnover pools and potentially reducing long-term C storage (*40*). Experiments and modeling analysis over longer timescales are therefore needed to resolve these uncertainties. Despite these limitations, the mechanistic understanding gained from this, alongside other manipulative experiments, offers invaluable insights into the future C fate of peatlands and can inform model improvements.

MATERIALS AND METHODS

Description of the experimental site

The SPRUCE experiment is located in the ombrotrophic S1 Bog, a perched water table peatland within the Marcell Experimental Forest, northern Minnesota, USA (47.5059°N, 93.4535°W). The mean annual temperature at the Marcell Experimental Forest was 3.4°C, and the average annual precipitation was 780 mm from 1961 to 2009, reflecting the area's boreal climate (*64*). The overstory vegetation is primarily composed of black spruce (*Picea mariana*) and tamarack (*Larix laricina*), underlain by a rich layer of *Sphagnum* spp. mosses (*Sphagnum divinum*, *Sphagnum angustifolium*, and *Sphagnum fallax*). The understory features a variety of shrubs like Labrador tea (*Rhododendron groenlandicum*), blueberry (*Vaccinium angustifolium*), and leatherleaf (*Chamaedaphne calyculata*), along with a few herbaceous and graminoid species (*11*). The peatland underwent strip cuts in 1969 and 1974 to test the effects of seeding on the natural regeneration of *P. mariana*. The current canopy stands at 5- to 8-m tall (*11*). The peatland soil is classified as the Greenwood series, a Typic Haplohemist (http://websoilsurvey.nrcs.usda.gov) (*65*), with accumulation dating back thousands of years to an average depth of 2 to 3 m (*66*).

The SPRUCE experiment is composed of 10 experimental plots, with each plot equipped with an open-top enclosure of 12.8-m diameter and 7-m tall. The regression design applies five distinct warming levels (+0°, +2.25°, +4.5°, +6.75°, and + 9°C) alongside two different CO_2 levels (+0 and + 500 ppm) to study their individual or interactive effects on peatland carbon (C) dynamics. Peatlands in high-latitude regions may experience warming of up to 8.3°C in the future (*7*, *8*). The temperature gradient at the experimental site (from +0° to +9°C) encompasses these potential warming scenarios. The design of gradient-based warming was intended to help better understand the sensitivity of peatland C cycling to increasing temperatures through regression analysis. Belowground warming of this experiment began in 2014 (*15*), followed by the commencement of whole-ecosystem warming in August 2015 (*11*). Belowground warming was achieved by strategically placing a series of low-wattage heaters to targeted depths (2- to 3-m deep), ensuring accurate temperature control. Air warming within the enclosures was achieved using propane-fired furnaces, which recirculated and heated the air. The elevated CO_2 treatment started in June 2016 to maintain the CO_2 concentration between 800 and 900 ppm (*11*). The warming treatments operated continuously throughout the year, while the elevated CO_2 treatments were applied during the growing season and daylight hours only.

Downloaded from https://www.science.org at Cornell University on October 30, 2026

Measurements

The measurements of 18 variables that were used to quantify peatland C fluxes and pools were collected in each of the 10 experimental plots, corresponding to 10 treatments at five levels of warming each under two levels of CO_2 concentration (a total of 180 variable-plot time series from 2011 to 2021) (table S1). Aboveground tree biomass was estimated using allometric relationships based on annual measurements of tree diameter at breast height (1.3 m) and periodic assessments of tree height (*67*). These measurements were then converted to C units, assuming that 48% of the tree's mass is C (*68*). Aboveground shrub-layer biomass was determined annually through destructive clipping (*69*). The area clipped in each experimental plot varied year to year but was typically 0.25 m^2. The clipped plant materials were divided into two categories: current year growth and older aboveground plant materials. These materials were then oven-dried at 70°C for several days and then weighed. The C content of all tissues, including leaves and stems, ranged from 46 to 53% (*59*). We used the mean measured values of 51.6% for leaves and 51.2% for stems. The annual growth of the *Sphagnum* community was measured in 3.8-cm-diameter mesh columns (*43*, *70*). The collected *Sphagnum* was oven-dried and weighed. The average C content of *Sphagnum* tissue was 42.9% (*70*). These measurements were combined with assessments of the *Sphagnum* community cover. The *Sphagnum* growth was estimated by the difference between mass measurements taken in May and October.

Fine-root biomass was measured using the minirhizotron method from 2015 to 2021. Two acrylic minirhizotron tubes (182.9-cm long, 5.08-cm inner diameter) were installed within 1.5 m of coniferous trees, one in a hummock and the other in an adjacent hollow. Plant root images were collected monthly using a BTC-100x minirhizotron camera (Bartz Technology Corporation, Carpinteria, CA, US) during the growing season. The images were processed using commercial software and classified into tree and shrub roots. Fine-root (less than 2 mm in diameter) production was estimated by measuring the length of new roots appearing between image collections and dividing by the days between the two observations. More details about fine-root measurements can be found in (*71*, *72*).

The measured biomass and C content were used to estimate the corresponding C pool sizes and calculate the annual NPP (g C m^{-2} $year^{-1}$) of different PFTs. Aboveground NPP (ANPP) of trees ($ANPP_{tree}$) was calculated from the difference in biomass between the current and previous years. Shrub ANPP ($ANPP_{shrub}$) was estimated from the measured new growth of stems and leaves during each year. *Sphagnum* NPP ($NPP_{Sphag.}$) was calculated from the annual growth measurements of *Sphagnum*, scaled by percent cover of *Sphagnum* community. Belowground NPP (BNPP) of shrubs and trees was assessed by the biomass of fine roots that grew during the current year.

CO_2 and methane (CH_4) fluxes were measured with the chambers placed on the in situ large collars (1.2-m diameter) within each enclosure. These collars contained shrub and *Sphagnum* species but not trees. A monthly measurement was taken during the growing season from day 122 of year to day 244 (*73*, *74*). Measurements of CO_2 fluxes were conducted with a LI-7500A (LI-COR, Lincoln, NB, US) under both light and dark conditions. Measurements in the light represented net CO_2 exchange in the collar, and dark measurements were used to estimate respiration in the large collar. The difference between these two measurements was used to estimate GPP of shrubs and *Sphagnum* ($GPP_{shrub} + GPP_{Sphag.}$) (*73*). Shrub LAI was measured using a LI-LAI-2200 (LI-COR, Lincoln, NB, US) from 2017 to 2019 (*75*). Tree GPP (GPP_{tree}) was estimated from tree leaf-level photosynthetic rates and LAI. The tree's leaf-level photosynthetic rates were measured using LI-6400XT and LI-6800 (LI-COR, Lincoln, NB, US) from 2016 to 2017 and 2019 for each plot (*76*, *77*). Tree LAI was estimated on the basis of annual maximum leaf mass and leaf mass per unit lamina area (LMA) from 2014 to 2021, with annual maximum leaf mass being estimated using allometric relationships (*78*).

Rh_{CO_2} was estimated as a proportion of total respiration. The proportion of Rh_{CO_2} to total respiration was measured in six pairs of dark collars with a 1.2-m diameter placed in an area adjacent to, but outside, the experimental plots. Each pair included one intact and another with all autotrophic vegetation removed. Each collar was embedded 10 to 20 cm into the surface peat. CO_2 emissions from each of these large collars were measured from 2017 to 2019. Differences in measured CO_2 emissions between intact and clipped collars from each pair were used to estimate the proportion of heterotrophic respiration to ecosystem respiration (0.40 ± 0.18) (*11*), with the remainder being attributed to Ra. CH_4 fluxes were measured by CH_4 sensors (Li-7700; LI-COR, Lincoln, NB, US) installed within the chambers of the in situ large collars within each experimental plot (*73*).

Soil C content was measured from peat core samples taken at each experimental plot in August 2012 and August 2020 (*79*). Three replicates of soil cores were collected from both hummock and hollow locations within each plot to depths of 2 to 3 m. Dry weight and C concentrations of soil samples were measured to determine soil C storage for each experimental plot.

Environmental variables were measured in each experimental plot (*80*). Air temperature and relative humidity were measured at 0.5, 1, 2, and 4 m above ground at half-hour intervals using thermistors (model HMP-155; Vaisala, Vantaa, Finland). Vapor pressure deficit was calculated from measured air temperature and relative humidity (*80*). Soil temperature in all plots was measured at a depth of 10 cm by multipoint thermistor probes (W.H. Cooke & Co. Inc., Hanover, PA). Photosynthetically active radiation was measured using LI-190R quantum sensors (LI-COR, Lincoln, NB, US) 2.5 m above the peat surface. Wind speed was measured by wind sensors (Windsonic 4; Gill Instruments, Lymington, UK) 10 m above each enclosure in the center. Other variables, including water table depth (2000-mm TruTrack Water and Temperature Voltage Output) and rainfall, were also recorded at half-hour intervals. These environmental data served as input data to drive the model.

Model-guided data synthesis approach

To estimate peatland C budgets under warming and eCO_2 across the 10 experimental plots, we applied a model-guided data synthesis approach in which a process-based model serves as a mechanistic framework to guide the synthesis and integration of 18 measured variables through a data assimilation technique. In this framework, the process-based model provides a mechanistic representation of ecosystem C cycling, while observational data constrain the model to ensure consistency between estimated and observed values. By combining mechanistic understanding of ecosystem processes with constrains from multiple observations, this approach generates internally consistent estimates of ecosystem C dynamics across different C pools and fluxes that cannot be directly quantified simultaneously through sparse measurements alone. In addition, the approach enables the integration of multiple ecosystem observations collected at different

Downloaded from https://www.science.org at Cornell University on October 30, 2026

temporal scales, including variables not directly related to ecosystem C budgets, into a unified framework for constraining ecosystem-scale C dynamics and their responses to warming and eCO_2.

The process-based model used in this study is a version of the TECO model specifically developed for the SPRUCE project (TECO-SPRUCE model). The original TECO model is designed to simulate biogeochemical cycles, canopy photosynthesis, plant growth, and water dynamics (*30*). To simulate peatland C cycling, TECO-SPRUCE has incorporated a soil thermal dynamic module (*81*) and a CH_4 module (*82*) into the original TECO model. In this study, we further modified the TECO-SPRUCE model to include three dominant PFTs: trees, shrubs, and *Sphagnum* (fig. S1). The TECO-SPRUCE model is driven by measured hourly meteorological data from each treatment.

We constrained the model using a Bayesian data assimilation approach that integrates observations with our process-based model. The approach uses a technique based on Bayes' Theorem for constraining parameters of a model. Its fundamental principle is Bayesian probabilistic inversion (*83*) that can be represented by

$$p(\theta \mid Z) \propto f(Z \mid \theta)\, p(\theta) \tag{1}$$

where $p(\theta|Z)$ is the posterior distribution of parameter θ, $f(Z|\theta)$ is the conditional probability density of observations Z given θ, and $p(\theta)$ represents the prior probability density function of parameter θ. In our research, we applied the Metropolis-Hastings algorithm (*84*) to generate the posterior distributions of model parameters. We set 50,000 iterations to derive the posterior distributions of parameters, with the acceptance ratios between 10 and 50%. The first half of the accepted parameter values were discarded as part of the burn-in period, and the second half were used for posterior analysis. We treated the initial states of C pools in the TECO-SPRUCE model as represented by parameters with prior ranges based on pretreatment measurements of biomass and soil C content from 2011 to 2013 (table S1). Then, we estimated the initial states and model parameters simultaneously from 18 observed variables for each experimental plot from 2011 to 2021 through a single round of data assimilation as was done in previous studies (*85*, *86*). To closely match the observations, we adopted a conditional inversion method to estimate parameter values yearly to reflect strong interannual variability in flux measurements (*87*). The optimized parameter values as shown in fig. S9 were used in simulations to estimate the C budgets across the 10 treatments. Further details on our data assimilation techniques have been elaborately discussed in the paper by Xu *et al.* (*83*).

Estimation of the carbon budget

We estimated the annual C budgets, including NCE, GPP, NPP, Ra, Rh_{CO_2}, and CH_4, from 2013 to 2021 using the constrained TECO-SPRUCE with 18 measured variables. The C budgets from 2017 to 2021 were used for the analysis of warming and elevated CO_2 impacts while the model outputs from 2014 to 2016 were not used due to partial treatments during these years. Treatment-induced changes in fluxes were all corrected for their differences with pretreatment values in 2013, which was estimated flux values during the treatment years (2017–2021) minus those in 2013 for each plot. This baseline correction accounted for pre-existing differences among plots, and its use was supported by the absence of significant nonlinear interactions between pretreatment conditions and warming or elevated CO_2 treatments in their effects on NCE, as assessed using linear mixed-effects models (fig. S11). Our NCE estimates represent the net C balance of the major ecosystem C fluxes explicitly quantified and constrained within the model-guided data synthesis framework and do not include lateral C fluxes, such as dissolved organic C and dissolved inorganic C, because of their relatively small magnitudes and the lack of significant warming effects under either ambient or elevated CO_2 (*11*). NCE was calculated from GPP of the three PFTs ($GPP_{tree} + GPP_{shrub} + GPP_{Sphag.}$), Ra ($Ra_{tree} + Ra_{shrub} + Ra_{Sphag.}$), and heterotrophic respiration (Rh_{CO_2} and CH_4) as below

$$NCE = GPP_{tree} + GPP_{shrub} + GPP_{Sphag.} - Ra_{tree} - Ra_{shrub} - Ra_{Sphag.} - Rh_{CO_2} - CH_4 \tag{2}$$

Modeling experiment

To assess the influence of ecosystem property changes induced by warming and elevated CO_2 on peatland C balance, we compared estimates from the TECO-SPRUCE model with fixed versus varying parameters. Specifically, we first conducted a modeling experiment in which C dynamics in all the 10 treatment plots were simulated using a single set of fixed parameters. These parameters were optimized with observations from the control treatment (i.e., +0°C and ambient CO_2) during the pretreatment period (2011–2013) and then applied them in the TECO-SPRUCE model to simulate all the 10 experimental plots during the treatment period (2014–2021) using plot-specific environmental data and initial C pool sizes. This approach is commonly used in simulation modeling to project ecosystem responses to climate change with fixed parameters. In contrast, parameter values that were optimized separately for each treatment via data assimilation with treatment-specific observations, as done in our study (i.e., varying parameters) were used to account for ecosystem property changes induced by warming and CO_2 treatments. This comparison allowed us to evaluate the importance of ecosystem property changes in regulating the C fate under climate change.

Supplementary Materials

This PDF file includes:

Figs. S1 to S11
Table S1
References

REFERENCES

1. S. Frolking, N. Roulet, J. Fuglestvedt, How northern peatlands influence the Earth's radiative budget: Sustained methane emission versus sustained carbon sequestration. *J. Geophys. Res.* **111**, G01008 (2006).
2. A. V. Gallego-Sala, D. J. Charman, S. Brewer, S. E. Page, I. C. Prentice, P. Friedlingstein, S. Moreton, M. J. Amesbury, D. W. Beilman, S. Björck, T. Blyakharchuk, C. Bochicchio, R. K. Booth, J. Bunbury, P. Camill, D. Carless, R. A. Chimner, M. Clifford, E. Cressey, C. Courtney-Mustaphi, F. De Vleeschouwer, R. de Jong, B. Fialkiewicz-Koziel, S. A. Finkelstein, M. Garneau, E. Githumbi, J. Hribjlan, J. Holmquist, P. D. M. Hughes, C. Jones, M. C. Jones, E. Karofeld, E. S. Klein, U. Kokfelt, A. Korhola, T. Lacourse, G. Le Roux, M. Lamentowicz, D. Large, M. Lavoie, J. Loisel, H. Mackay, G. M. MacDonald, M. Makila, G. Magnan, R. Marchant, K. Marcisz, A. M. Cortizas, C. Massa, P. Mathijssen, D. Mauquoy, T. Mighall, F. J. G. Mitchell, P. Moss, J. Nichols, P. O. Oksanen, L. Orme, M. S. Packalen, S. Robinson, T. P. Roland, N. K. Sanderson, A. B. K. Sannel, N. Silva-Sánchez, N. Steinberg, G. T. Swindles, T. E. Turner, J. Uglow, M. Väliranta, S. van Bellen, M. van der Linden, B. van Geel, G. P. Wang, Z. C. Yu, J. Zaragoza-Castells, Y. Zhao, Latitudinal limits to the predicted increase of the peatland carbon sink with warming. *Nat. Clim. Change* **8**, 907–913 (2018).
3. C. C. Treat, T. Kleinen, N. Broothaerts, A. S. Dalton, R. Dommain, T. A. Douglas, J. Z. Drexler, S. A. Finkelstein, G. Grosse, G. Hope, J. Hutchings, M. C. Jones, P. Kuhry, T. Lacourse, O. Lähteenoja, J. Loisel, B. Notebaert, R. J. Payne, D. M. Peteet, A. B. K. Sannel, J. M. Stelling, J. Strauss, G. T. Swindles, J. Talbot, C. Tarnocai, G. Verstraeten, C. J. Williams, Z. Y. Xia, Z. C. Yu, M. Väliranta, M. Hättestrand, H. Alexanderson, V. Brovkin, Widespread global peatland establishment and persistence over the last 130,000 y. *Proc. Natl. Acad. Sci. U.S.A.* **116**, 4822–4827 (2019).

Downloaded from https://www.science.org at Cornell University on October 30, 2026

4. J. Loisel, A. V. Gallego-Sala, M. J. Amesbury, G. Magnan, G. Anshari, D. W. Beilman, J. C. Benavides, J. Blewett, P. Camill, D. J. Charman, S. Chawchai, A. Hedgpeth, T. Kleinen, A. Korhola, D. Large, C. A. Mansilla, J. Müller, S. van Bellen, J. B. West, Z. Yu, J. L. Bubier, M. Garneau, T. Moore, A. B. K. Sannel, S. Page, M. Väliranta, M. Bechtold, V. Brovkin, L. E. S. Cole, J. P. Chanton, T. R. Christensen, M. A. Davies, F. De Vleeschouwer, S. A. Finkelstein, S. Frolking, M. Galka, L. Gandois, N. Girkin, L. I. Harris, A. Heinemeyer, A. M. Hoyt, M. C. Jones, F. Joos, S. Juutinen, K. Kaiser, T. Lacourse, M. Lamentowicz, T. Larmola, J. Leifeld, A. Lohila, A. M. Milner, K. Minkkinen, P. Moss, B. D. A. Naafs, J. Nichols, J. O'Donnell, R. Payne, M. Philben, S. Piilo, A. Quillet, A. S. Ratnayake, T. P. Roland, S. Sjögersten, O. Sonnentag, G. T. Swindles, W. Swinnen, J. Talbot, C. Treat, A. C. Valach, J. Wu, Expert assessment of future vulnerability of the global peatland carbon sink. *Nat. Clim. Change* **11**, 70–77 (2021).
5. Z. Yu, J. Loisel, D. P. Brosseau, D. W. Beilman, S. J. Hunt, Global peatland dynamics since the Last Glacial Maximum. *Geophys. Res. Lett.* **37**, L13402 (2010).
6. S. D. Bridgham, J. P. Megonigal, J. K. Keller, N. B. Bliss, C. Trettin, The carbon balance of North American wetlands. *Wetlands* **26**, 889–916 (2006).
7. C. Schädel, M. K. F. Bader, E. A. G. Schuur, C. Biasi, R. Bracho, P. Čapek, S. De Baets, K. Diáková, J. Ernakovich, C. Estop-Aragones, D. E. Graham, I. P. Hartley, C. M. Iversen, E. S. Kane, C. Knoblauch, M. Lupascu, P. J. Martikainen, S. M. Natali, R. J. Norby, J. A. O'Donnell, T. R. Chowdhury, H. Šantrůčková, G. Shaver, V. L. Sloan, C. C. Treat, M. R. Turetsky, M. P. Waldrop, K. P. Wickland, Potential carbon emissions dominated by carbon dioxide from thawed permafrost soils. *Nat. Clim. Change* **6**, 950–953 (2016).
8. M. Collins, F. S. Thomas, D. Qin, G.-K. Plattner, M. Tignor, S. K. Allen, J. Boschung, A. Nauels, Y. Xia, V. Bex, in *Climate Change 2013: The Physical Science Basis*, T. F. Stocker, D. Qin, G.-K. Plattner, M. M. B. Tignor, S. K. Allen, J. Boschung, A. Nauels, Y. Xia, V. Bex, P. M. Midgley, eds, (IPCC, Cambridge Univ. Press, 2013), pp. 1029–1136.
9. M. Helbig, T. Zivkovic, P. Alekseychik, M. Aurela, T. S. El-Madany, E. S. Euskirchen, L. B. Flanagan, T. J. Griffis, P. J. Hanson, J. Hattakka, C. Helfter, T. Hirano, E. R. Humphreys, G. Kiely, R. K. Kolka, T. Laurila, P. G. Leahy, A. Lohila, I. Mammarella, M. B. Nilsson, A. Panov, F. J. W. Parmentier, M. Peichl, J. Rinne, D. T. Roman, O. Sonnentag, E.-S. Tuittila, M. Ueyama, T. Vesala, P. Vestin, S. Weldon, P. Weslien, S. Zaehle, Warming response of peatland CO_2 sink is sensitive to seasonality in warming trends. *Nat. Clim. Change* **12**, 743–749 (2022).
10. A. M. Hopple, R. M. Wilson, M. Kolton, C. A. Zalman, J. P. Chanton, J. Kostka, P. J. Hanson, J. K. Keller, S. D. Bridgham, Massive peatland carbon banks vulnerable to rising temperatures. *Nat. Commun.* **11**, 2373 (2020).
11. P. J. Hanson, N. A. Griffiths, C. M. Iversen, R. J. Norby, S. D. Sebestyen, J. R. Phillips, J. P. Chanton, R. K. Kolka, A. Malhotra, K. C. Oleheiser, J. M. Warren, X. Y. Shi, X. J. Yang, J. F. Mao, D. M. Ricciuto, Rapid net carbon loss from a whole-ecosystem warmed peatland. *AGU Adv.* **1**, e2020AV000163 (2020).
12. N. Chaudhary, S. Westermann, S. Lamba, N. Shurpali, B. K. Sannel, G. Schurgers, P. A. Miller, B. Smith, Modelling past and future peatland carbon dynamics across the pan-Arctic. *Glob. Change Biol.* **26**, 4119–4133 (2020).
13. C. Terrer, R. P. Phillips, B. A. Hungate, J. Rosende, J. Pett-Ridge, M. E. Craig, K. J. van Groenigen, T. F. Keenan, B. N. Sulman, B. D. Stocker, P. B. Reich, A. F. A. Pellegrini, E. Pendall, H. Zhang, R. D. Evans, Y. Carrillo, J. B. Fisher, K. Van Sundert, S. Vicca, R. B. Jackson, A trade-off between plant and soil carbon storage under elevated CO_2. *Nature* **591**, 599–603 (2021).
14. J. Leifeld, C. Wüst-Galley, S. Page, Intact and managed peatland soils as a source and sink of GHGs from 1850 to 2100. *Nat. Clim. Change* **9**, 945–947 (2019).
15. R. M. Wilson, A. M. Hopple, M. M. Tfaily, S. D. Sebestyen, C. W. Schadt, L. Pfeifer-Meister, C. Medvedeff, K. J. McFarlane, J. E. Kostka, M. Kolton, R. K. Kolka, L. A. Kluber, J. K. Keller, T. P. Guilderson, N. A. Griffiths, J. P. Chanton, S. D. Bridgham, P. J. Hanson, Stability of peatland carbon to rising temperatures. *Nat. Commun.* **7**, 13723 (2016).
16. E. A. Davidson, I. A. Janssens, Temperature sensitivity of soil carbon decomposition and feedbacks to climate change. *Nature* **440**, 165–173 (2006).
17. Y. Q. Luo, S. Q. Wan, D. F. Hui, L. L. Wallace, Acclimatization of soil respiration to warming in a tall grass prairie. *Nature* **413**, 622–625 (2001).
18. J. Liang, J. Xia, Z. Shi, L. Jiang, S. Ma, X. J. Lu, M. Mauritz, S. M. Natali, E. Pegoraro, C. R. Penton, C. Plaza, V. G. Salmon, G. Celis, J. R. Cole, K. T. Konstantinidis, J. M. Tiedje, J. Z. Zhou, E. A. G. Schuur, Y. Luo, Biotic responses buffer warming-induced soil organic carbon loss in Arctic tundra. *Glob. Change Biol.* **24**, 4946–4959 (2018).
19. Y. Luo, B. Su, W. S. Currie, J. S. Dukes, A. Finzi, U. Hartwig, B. Hungate, R. E. McMurtrie, R. Oren, W. J. Parton, D. E. Pataki, R. M. Shaw, D. R. Zak, C. B. Field, Progressive nitrogen limitation of ecosystem responses to rising atmospheric carbon dioxide. *Bioscience* **54**, 731–739 (2004).
20. Y. Luo, S. Niu, The fertilization effect of CO_2 on a mature forest. *Nature* **580**, 191–192 (2020).
21. Q. Li, X. Lu, Y. Wang, X. Huang, P. M. Cox, Y. Luo, Leaf area index identified as a major source of variability in modeled CO_2 fertilization. *Biogeosciences* **15**, 6909–6925 (2018).
22. J. M. Chen, W. Ju, P. Ciais, N. Viovy, R. Liu, Y. Liu, X. Lu, Vegetation structural change since 1981 significantly enhanced the terrestrial carbon sink. *Nat. Commun.* **10**, 4259 (2019).
23. K. Yue, D. A. Fornara, W. Yang, Y. Peng, C. Peng, Z. Liu, F. Wu, Influence of multiple global change drivers on terrestrial carbon storage: Additive effects are common. *Ecol. Lett.* **20**, 663–672 (2017).
24. J. Song, S. Wan, S. Piao, A. K. Knapp, A. T. Classen, S. Vicca, P. Ciais, M. J. Hovenden, S. Leuzinger, C. Beier, P. Kardol, J. Xia, Q. Liu, J. Ru, Z. Zhou, Y. Luo, D. Guo, J. A. Langley, J. Zscheischler, J. S. Dukes, J. Tang, J. Chen, K. S. Hofmockel, L. M. Kueppers, L. Rustad, L. Liu, M. D. Smith, P. H. Templer, R. Q. Thomas, R. J. Norby, R. P. Phillips, S. Niu, S. Fatichi, Y. Wang, P. Shao, H. Han, D. Wang, L. Lei, J. Wang, X. Li, Q. Zhang, X. Li, F. Su, B. Liu, F. Yang, G. Ma, G. Li, Y. Liu, Y. Liu, Z. Yang, K. Zhang, Y. Miao, M. Hu, C. Yan, A. Zhang, M. Zhong, Y. Hui, Y. Li, M. Zheng, A meta-analysis of 1,119 manipulative experiments on terrestrial carbon-cycling responses to global change. *Nat. Ecol. Evol.* **3**, 1309–1320 (2019).
25. M. Olsrud, B. Å. Carlsson, B. M. Svensson, A. Michelsen, J. M. Melillo, Responses of fungal root colonization, plant cover and leaf nutrients to long-term exposure to elevated atmospheric CO_2 and warming in a subarctic birch forest understory. *Glob. Change Biol.* **16**, 1820–1829 (2010).
26. P. J. Hanson, J. S. Riggs, W. R. Nettles, J. R. Phillips, M. B. Krassovski, L. A. Hook, L. H. Gu, A. D. Richardson, D. M. Aubrecht, D. M. Ricciuto, J. M. Warren, C. Barbier, Attaining whole-ecosystem warming using air and deep-soil heating methods with an elevated CO_2 atmosphere. *Biogeosciences* **14**, 861–883 (2017).
27. M. B. Krassovski, J. S. Riggs, L. A. Hook, W. R. Nettles, P. J. Hanson, T. A. Boden, A comprehensive data acquisition and management system for an ecosystem-scale peatland warming and elevated CO_2 experiment. *Geosci. Instrum. Meth.* **4**, 203–213 (2015).
28. F. Tao, Y. Y. Huang, B. A. Hungate, S. Manzoni, S. D. Frey, M. W. I. Schmidt, M. Reichstein, N. Carvalhais, P. Ciais, L. F. Jiang, J. Lehmann, Y. P. Wang, B. Z. Houlton, B. Ahrens, U. Mishra, G. Hugelius, T. D. Hocking, X. J. Lu, Z. Shi, K. Viatkin, R. Vargas, Y. Yigini, C. Omuto, A. A. Malik, G. Peralta, R. Cuevas-Corona, L. E. Di Paolo, I. Luotto, C. J. Liao, Y. S. Liang, V. S. Saynes, X. M. Huang, Y. Q. Luo, Microbial carbon use efficiency promotes global soil carbon storage. *Nature* **618**, 981–985 (2023).
29. M. Jiang, B. E. Medlyn, J. E. Drake, R. A. Duursma, I. C. Anderson, C. V. M. Barton, M. M. Boer, Y. Carrillo, L. Castaneda-Gomez, L. Collins, K. Y. Crous, M. G. De Kauwe, B. M. dos Santos, K. M. Emmerson, S. L. Facey, A. N. Gherlenda, T. E. Gimeno, S. Hasegawa, S. N. Johnson, A. Kannaste, C. A. Macdonald, K. Mahmud, B. D. Moore, L. Nazaries, E. H. J. Neilson, U. N. Nielsen, U. Niinemets, N. J. Noh, R. Ochoa-Hueso, V. S. Pathare, E. Pendall, J. Pihlblad, J. Pineiro, J. R. Powell, S. A. Power, P. B. Reich, A. A. Renchon, M. Riegler, R. Rinnan, P. D. Rymer, R. L. Salomon, B. K. Singh, B. Smith, M. G. Tjoelker, J. K. M. Walker, A. Wujeska-Klause, J. Y. Yang, S. Zaehle, D. S. Ellsworth, The fate of carbon in a mature forest under carbon dioxide enrichment. *Nature* **580**, 227–231 (2020).
30. E. S. Weng, Y. Q. Luo, Soil hydrological properties regulate grassland ecosystem responses to multifactor global change: A modeling analysis. *J. Geophys. Res. Biogeosci.* **113**, G0539 (2008).
31. S. Ma, L. Jiang, R. M. Wilson, J. Chanton, S. Niu, C. M. Iversen, A. Malhotra, J. Jiang, Y. Huang, X. Lu, Thermal acclimation of plant photosynthesis and autotrophic respiration in a northern peatland. *Environ. Res. Clim.* **2**, 025003 (2023).
32. R. J. Norby, T. Baxter, T. Živković, D. J. Weston, Shading contributes to *Sphagnum* decline in response to warming. *Ecol. Evol.* **13**, e10542 (2023).
33. E. H. DeLucia, J. E. Drake, R. B. Thomas, M. Gonzalez-Meler, Forest carbon use efficiency: Is respiration a constant fraction of gross primary production? *Glob. Change Biol.* **13**, 1157–1167 (2007).
34. M. R. Shaw, E. S. Zavaleta, N. R. Chiariello, E. E. Cleland, H. A. Mooney, C. B. Field, Grassland responses to global environmental changes suppressed by elevated CO_2. *Science* **298**, 1987–1990 (2002).
35. Y. Kuzyakov, Priming effects: Interactions between living and dead organic matter. *Soil Biol. Biochem.* **42**, 1363–1371 (2010).
36. K. J. Van Groenigen, X. Qi, C. W. Osenberg, Y. Luo, B. A. Hungate, Faster decomposition under increased atmospheric CO_2 limits soil carbon storage. *Science* **344**, 508–509 (2014).
37. C. M. Iversen, J. Latimer, D. J. Brice, J. Childs, H. M. Vander Stel, C. E. Defrenne, J. Graham, N. A. Griffiths, A. Malhotra, R. J. Norby, K. C. Oleheiser, J. R. Phillips, V. G. Salmon, S. D. Sebestyen, X. J. Yang, P. J. Hanson, Whole-ecosystem warming increases plant-available nitrogen and phosphorus in an ombrotrophic bog. *Ecosystems* **26**, 86–113 (2023).
38. Q. Quan, J. Zhou, P. J. Hanson, D. Ricciuto, S. D. Sebestyen, D. J. Weston, J. P. Chanton, R. M. Wilson, J. E. Kostka, Y. Zhou, N. Wei, L. Jiang, M. A. Mayes, J. M. Stelling, A. D. Richardson, M. E. Dusenge, D. Way, J. M. Warren, Y. Luo, Drought-induced peatland carbon loss exacerbated by elevated CO_2 and warming. *Science* **390**, 367–370 (2025).
39. Y. Huang, P. Ciais, Y. Luo, D. Zhu, Y. Wang, C. Qiu, D. S. Goll, B. Guenet, D. Makowski, I. De Graaf, Tradeoff of CO_2 and CH_4 emissions from global peatlands under water-table drawdown. *Nat. Clim. Change* **11**, 618–622 (2021).
40. N. O. E. Ofiti, M. W. I. Schmidt, S. Abiven, P. J. Hanson, C. M. Iversen, R. M. Wilson, J. E. Kostka, G. L. B. Wiesenberg, A. Malhotra, Climate warming and elevated CO_2 alter peatland soil carbon sources and stability. *Nat. Commun.* **14**, 7533 (2023).

Downloaded from https://www.science.org at Cornell University on October 30, 2026

41. E. J. Ward, J. M. Warren, D. A. McLennan, M. E. Dusenge, D. A. Way, S. D. Wullschleger, P. J. Hanson, Photosynthetic and respiratory responses of two bog shrub species to whole ecosystem warming and elevated CO_2 at the boreal-temperate ecotone. *Front. For. Glob. Chang.* **2**, 54 (2019).
42. M. Y. McPartland, R. A. Montgomery, P. J. Hanson, J. R. Phillips, R. Kolka, B. Palik, Vascular plant species response to warming and elevated carbon dioxide in a boreal peatland. *Environ. Res. Lett.* **15**, 124066 (2020).
43. R. J. Norby, J. Childs, P. J. Hanson, J. M. Warren, Rapid loss of an ecosystem engineer: *Sphagnum* decline in an experimentally warmed bog. *Ecol. Evol.* **9**, 12571–12585 (2019).
44. H. J. Wang, J. Q. Tian, H. Chen, M. C. Ho, R. Vilgalys, Z. J. Bu, X. Z. Liu, C. J. Richardson, Vegetation and microbes interact to preserve carbon in many wooded peatlands. *Commun. Earth Environ.* **2**, 67 (2021).
45. Y. Luo, E. A. G. Schuur, Model parameterization to represent processes at unresolved scales and changing properties of evolving systems. *Glob. Change Biol.* **26**, 1109–1117 (2020).
46. S. D. Allison, A trait-based approach for modelling microbial litter decomposition. *Ecol. Lett.* **15**, 1058–1070 (2012).
47. D. C. Laughlin, Applying trait-based models to achieve functional targets for theory-driven ecological restoration. *Ecol. Lett.* **17**, 771–784 (2014).
48. W. Chen, S. Wang, J. Wang, J. Xia, Y. Luo, G. Yu, S. Niu, Evidence for widespread thermal optimality of ecosystem respiration. *Nat. Ecol. Evol.* **7**, 1379–1387 (2023).
49. X. Xu, J. Li, X. Li, C. Fang, B. Li, M. Nie, Thermal adaptation of respiration in terrestrial ecosystems alleviates carbon loss. *Nat. Clim. Change* **15**, 873–879 (2025).
50. N. Fenner, C. Freeman, Drought-induced carbon loss in peatlands. *Nat. Geosci.* **4**, 895–900 (2011).
51. M. R. Turetsky, B. Benscoter, S. Page, G. Rein, G. R. van der Werf, A. Watts, Global vulnerability of peatlands to fire and carbon loss. *Nat. Geosci.* **8**, 11–14 (2015).
52. M. Y. McPartland, E. S. Kane, M. J. Falkowski, R. Kolka, M. R. Turetsky, B. Palik, R. A. Montgomery, The response of boreal peatland community composition and NDVI to hydrologic change, warming, and elevated carbon dioxide. *Glob. Change Biol.* **25**, 93–107 (2019).
53. J. Song, S. Wan, S. Piao, D. Hui, M. J. Hovenden, P. Ciais, Y. Liu, Y. Liu, M. Zhong, M. Zheng, G. Ma, Z. Zhou, J. Ru, Elevated CO_2 does not stimulate carbon sink in a semi-arid grassland. *Ecol. Lett.* **22**, 458–468 (2019).
54. Z. Chen, W. Wang, G. Forzieri, A. Cescatti, Transition from positive to negative indirect CO_2 effects on the vegetation carbon uptake. *Nat. Commun.* **15**, 1500 (2024).
55. S. Chen, Y. Zhang, Q. Wu, S. Liu, C. Song, J. Xiao, L. E. Band, J. M. Vose, Vegetation structural change and CO_2 fertilization more than offset gross primary production decline caused by reduced solar radiation in China. *Agric. For. Meteorol.* **296**, 108207 (2021).
56. M. Kovenock, A. L. Swann, Leaf trait acclimation amplifies simulated climate warming in response to elevated carbon dioxide. *Global Biogeochem. Cycles* **32**, 1437–1448 (2018).
57. J. Kim, L. Rochefort, S. Hogue-Hugron, Z. Alqulaiti, C. Dunn, R. Pouliot, T. G. Jones, C. Freeman, H. Kang, Water table fluctuation in peatlands facilitates fungal proliferation, impedes *Sphagnum* growth and accelerates decomposition. *Front. Earth Sci.* **8**, 579329 (2021).
58. E. Köster, J. P. Chapman, J. M. Barel, A. Korrensalo, A. M. Laine, H. T. Vasander, E. S. Tuittila, Water level drawdown makes boreal peatland vegetation more responsive to weather conditions. *Glob. Change Biol.* **29**, 5691–5705 (2023).
59. P. J. Hanson, N. A. Griffiths, V. G. Salmon, J. M. Birkebak, J. M. Warren, J. R. Phillips, M. P. Guilliams, K. C. Oleheiser, M. W. Jones, N. J. Jones, Peatland plant community changes in annual production and composition through 8 years of warming manipulations under ambient and elevated CO_2 atmospheres. *J. Geophys. Res. Biogeosci.* **130**, e2024JG008511 (2025).
60. J. Xia, J. Chen, S. Piao, P. Ciais, Y. Luo, S. Wan, Terrestrial carbon cycle affected by non-uniform climate warming. *Nat. Geosci.* **7**, 173–180 (2014).
61. K. L. Griffin, D. Sims, J. Seemann, Altered night-time CO_2 concentration affects the growth, physiology and biochemistry of soybean. *Plant Cell Environ.* **22**, 91–99 (1999).
62. S. Wang, Y. Zhang, W. Ju, J. M. Chen, P. Ciais, A. Cescatti, J. Sardans, I. A. Janssens, M. Wu, J. A. Berry, Recent global decline of CO_2 fertilization effects on vegetation photosynthesis. *Science* **370**, 1295–1300 (2020).
63. E. A. Ainsworth, S. P. Long, What have we learned from 15 years of free-air CO_2 enrichment (FACE)? A meta-analytic review of the responses of photosynthesis, canopy properties and plant production to rising CO_2. *New Phytol.* **165**, 351–372 (2005).
64. S. D. Sebestyen, C. Dorrance, D. M. Olson, E. S. Verry, R. K. Kolka, A. E. Elling, R. Kyllander, "Long-term monitoring sites and trends at the Marcell Experimental Forest," in *Peatland Biogeochemistry and Watershed Hydrology at the Marcell Experimental Forest*, vol 1., pp. 15–71 (2011).
65. A. D. Parsekian, L. Slater, D. Ntarlagiannis, J. Nolan, S. D. Sebesteyen, R. K. Kolka, P. J. Hanson, Uncertainty in peat volume and soil carbon estimated using ground-penetrating radar and probing. *Soil Sci. Soc. Am. J.* **76**, 1911–1918 (2012).
66. K. J. McFarlane, P. J. Hanson, C. M. Iversen, J. R. Phillips, D. J. Brice, Local spatial heterogeneity of Holocene carbon accumulation throughout the peat profile of an ombrotrophic Northern Minnesota bog. *Radiocarbon* **60**, 941–962 (2018).
67. P. J. Hanson, J. R. Phillips, S. D. Wullschleger, W. R. Nettles, J. M. Warren, E. J. Ward, J. D. Graham, T. A. Ruggles, SPRUCE tree growth assessments of Picea and Larix in S1-Bog plots and SPRUCE experimental plots, beginning in 2011 (Oak Ridge National Laboratory, TES SFA, US Department of Energy, 2018); https://doi.org/10.25581/spruce.051/1433836.
68. N. A. Griffiths, P. J. Hanson, D. M. Ricciuto, C. M. Iversen, A. M. Jensen, A. Malhotra, K. J. McFarlane, R. J. Norby, K. Sargsyan, S. D. Sebestyen, Temporal and spatial variation in peatland carbon cycling and implications for interpreting responses of an ecosystem-scale warming experiment. *Soil Sci. Soc. Am. J.* **81**, 1668–1688 (2017).
69. P. Hanson, J. Phillips, D. Brice, L. Hook, SPRUCE shrub-layer growth assessments in S1-Bog plots and SPRUCE experimental plots beginning in 2010. (Oak Ridge National Laboratory, TES SFA, US Department of Energy, 2018); https://doi.org/10.25581/spruce.052/1433837.
70. R. Norby, J. Childs, SPRUCE: *Sphagnum* productivity and community composition in the SPRUCE experimental plots (Oak Ridge National Laboratory, TES SFA, US Department of Energy, 2018); https://doi.org/10.25581/spruce.049/1426474.
71. S. E. Weber, J. Childs, J. Latimer, P. J. Hanson, V. G. Salmon, G. Schwaner, C. M. Iversen, Fine-root responses to warming and elevated CO_2 vary among plant functional types. *J. Ecol.* **114**, e70408 (2026).
72. S. E. Weber, J. Childs, J. M. Latimer, V. G. Salmon, G. Schwaner, C. M. Iversen, SPRUCE Root Production Assessed with Manual Minirhizotrons Resolved to Plant Functional Type, 2015–2021 (Oak Ridge National Laboratory, TES SFA, US Department of Energy, 2025); https://doi.org/10.25581/spruce.127/2570059.
73. P. Hanson, A. Gill, X. Xu, J. Phillips, D. Weston, R. Kolka, J. Riggs, L. Hook, Intermediate-scale community-level flux of CO_2 and CH_4 in a Minnesota peatland: Putting the SPRUCE project in a global context. *Biogeochemistry* **129**, 255–272 (2016).
74. P. Hanson, J. Phillips, J. Riggs, W. Nettles, SPRUCE Large-Collar in Situ CO2 and CH4 Flux Data for the SPRUCE Experimental Plots: Whole-Ecosystem-Warming (Oak Ridge National Laboratory, TES SFA, US Department of Energy, 2017); https://doi.org/10.3334/cdiac/spruce.034.
75. M. McPartland, E. Kane, M. Falkowski, R. Kolka, M. Turetsky, B. Palik, R. Montgomery, SPRUCE: LAI Data from SPRUCE Experimental Plots, 2017–2019 (Oak Ridge National Laboratory, TES SFA, US Department of Energy, 2019); https://doi.org/10.25581/spruce.058/1491566.
76. M. E. Dusenge, E. Ward, J. Warren, D. McLennan, J. Stinziano, B. Murphy, A. King, J. Childs, D. Brice, J. Phillips, SPRUCE Photosynthesis and Respiration of *Picea mariana and Larix laricina* in SPRUCE Experimental Plots, 2016–2017 (Oak Ridge National Laboratory, TES SFA, US Department of Energy, 2020); https://doi.org/10.25581/spruce.056/1455138.
77. M. E. Balog, J. Hauger, D. A. McLennan, J. M. Peters, J. M. Warren, SPRUCE Photosynthesis and Respiration of *Picea mariana and Larix laricina* in SPRUCE Experimental Plots, 2019 (Oak Ridge National Laboratory, TES SFA, US Department of Energy, 2025); https://doi.org/10.25581/spruce.121/2503934.
78. P. Hanson, D. Brice, C. Garten, L. Hook, J. Phillips, D. Todd, SPRUCE S1 Bog Vegetation Allometric and Biomass Data: 2010-2011 (Oak Ridge National Laboratory, TES SFA, US Department of Energy, 2012); https://doi.org/10.3334/CDIAC/spruce.004.
79. J. Phillips, P. Hanson, K. McFarlane, S. P. Participants, SPRUCE Peat Physical and Chemical Characteristics from Experimental Plot Cores, Select Pre-Treatment 2012 and Post-treatment 2020–2021 (Oak Ridge National Laboratory, TES SFA, US Department of Energy, 2022); https://doi.org/10.25581/spruce.102/1878603.
80. P. Hanson, J. Riggs, W. R. Nettles, M. Krassovski, L. Hook, SPRUCE whole ecosystems warming (WEW) environmental data beginning August 2015 (Oak Ridge National Laboratory, TES SFA, US Department of Energy, 2016); https://doi.org/10.3334/CDIAC/spruce.032.
81. Y. Huang, J. Jiang, S. Ma, D. Ricciuto, P. J. Hanson, Y. Luo, Soil thermal dynamics, snow cover, and frozen depth under five temperature treatments in an ombrotrophic bog: Constrained forecast with data assimilation. *J. Geophys. Res. Biogeosci.* **122**, 2046–2063 (2017).
82. S. Ma, J. Jiang, Y. Huang, Z. Shi, R. M. Wilson, D. Ricciuto, S. D. Sebestyen, P. J. Hanson, Y. Luo, Data-constrained projections of methane fluxes in a northern Minnesota peatland in response to elevated CO_2 and warming. *J. Geophys. Res. Biogeosci.* **122**, 2841–2861 (2017).
83. T. Xu, L. White, D. Hui, Y. Luo, Probabilistic inversion of a terrestrial ecosystem model: Analysis of uncertainty in parameter estimation and model prediction. *Global Biogeochem. Cycles* **20**, GB002468 (2006).
84. N. Metropolis, A. W. Rosenbluth, M. N. Rosenbluth, A. H. Teller, E. Teller, Equation of state calculations by fast computing machines. *J. Chem. Phys.* **21**, 1087–1092 (1953).
85. P. Peylin, C. Bacour, N. MacBean, S. Leonard, P. Rayner, S. Kuppel, E. Koffi, A. Kane, F. Maignan, F. Chevallier, P. Ciais, P. Prunet, A new stepwise carbon cycle data assimilation system using multiple data streams to constrain the simulated land surface carbon cycle. *Geosci. Model Dev.* **9**, 3321–3346 (2016).
86. E. Weng, Y. Luo, Relative information contributions of model vs. data to short-and long-term forecasts of forest carbon dynamics. *Ecol. Appl.* **21**, 1490–1505 (2011).
87. X. Wu, Y. Luo, E. Weng, L. White, Y. Ma, X. Zhou, Conditional inversion to estimate parameters from eddy-flux observations. *J. Plant Ecol.* **2**, 55–68 (2009).

Downloaded from https://www.science.org at Cornell University on October 30, 2026

88. M. McPartland, M. Falkowski, R. Kolka, M. Turetsky, B. Palik, R. Montgomery, SPRUCE: Vegetation community survey data from SPRUCE experimental plots, 2014–2018 (Oak Ridge National Laboratory, TES SFA, US Department of Energy, 2018); https://doi.org/10.25581/spruce.059/1499107.

Acknowledgments: We thank the SPRUCE project team for the efforts in experimental management and maintenance to support this study and all researchers involved in contributing data to the SPRUCE project databases. **Funding:** This material is based on work supported by the US Department of Energy, Office of Science, Office of Biological and Environmental Research. Oak Ridge National Laboratory is managed by UT-Battelle, LLC, for the US Department of Energy under contract DE-AC05-00OR22725. This work was also supported by grants awarded to Y.L. as follows: US Department of Energy (DE-AC05-1008 00OR22725), US Department of Energy (DE-SC0023514), US Department of Agriculture National Institute of Food and Agriculture (NIFA), the US National Science Foundation National AI Research Institutes Competitive Award (no. 2023-67021-39829), then US National Science Foundation (DEB 2406930 and DEB 2425290), and The project NYS Connects: Advancing Markets for Producers funded by US Department of Agriculture (USDA) and New York State Department of Environmental Conservation. **Author contributions:** Conceptualization: Y.L., W.H., J.Z., Q.Q., J.M.W., N.A.G., P.J.H., and D.R. Formal analysis: J.Z., F.T., and W.C. Writing—original draft: J.Z., W.H., and Y.L. Writing—review and editing: J.Z., Y.L., Q.Q., F.T., M.E.D., L.J., R.J.N., Yu Z., J.M.W., N.A.G., S.E.W., H.X., P.J.H., V.G.S., X.S., M.Y.M., W.H., D.W., D.R., M.A.M., and Ya.Z. Project administration: P.J.H., D.R., M.A.M., J.M.W., N.A.G., Y.L., J.Z., and V.G.S. Methodology: J.Z., Y.L., Q.Q., Yu Z., J.M.W., N.A.G., H.X., and P.J.H. Investigation: P.J.H., M.A.M., J.Z., M.E.D., R.J.N., J.M.W., N.A.G., V.G.S., Q.Q., S.E.W., X.S., and M.Y.M. Data curation: M.E.D., J.M.W., N.A.G., J.Z., S.E.W., P.J.H., and V.G.S. Validation: Y.L., J.Z., F.T., M.E.D., and V.G.S. Resources: Y.L., J.Z., J.M.W., W.C., and D.W. Funding acquisition: Y.L., J.M.W., S.E.W., P.J.H., V.G.S., and D.R. Supervision: Y.L., J.M.W., J.Z., S.E.W., D.W., and D.R. Software: J.Z. Visualization: J.Z., Y.L., S.E.W., V.G.S., and W.C. **Competing interests:** The authors declare that they have no competing interests. **Data, code, and materials availability:** All data and code needed to evaluate and reproduce the results in the paper are present in the paper and/or the Supplementary Materials. This study did not generate new materials. The raw data sets used in this study are available in the online SPRUCE project and for long-term storage in the US Department of Energy's (DOE) Environmental System Science Data Infrastructure for a Virtual Ecosystem (ESS-DIVE). The primary datasets used in this study are publicly available at the following permanent DOI links: SPRUCE shrub-layer growth assessments (https://doi.org/10.25581/spruce.052/1433837); SPRUCE tree growth assessments of Picea and Larix (https://doi.org/10.25581/spruce.051/1433836); SPRUCE *Sphagnum* productivity and community composition (https://doi.org/10.25581/spruce.049/1426474); SPRUCE peat physical and chemical characteristics (https://doi.org/10.25581/spruce.102/1878603); SPRUCE root production resolved to PFT (https://doi.org/10.25581/spruce.127/2570059); SPRUCE large-collar in situ CO_2 and CH_4 fluxes (https://doi.org/10.3334/cdiac/spruce.034); SPRUCE LAI data (https://doi.org/10.25581/spruce.058/1491566); SPRUCE photosynthesis and respiration of *P. mariana* and *L. laricina*, 2016–2017 (https://doi.org/10.25581/spruce.056/1455138); and SPRUCE photosynthesis and respiration of *P. mariana* and *L. laricina*, 2019 (https://doi.org/10.25581/spruce.121/2503934). The processed data and code used directly for the analyses and figures in this study are archived in the Dryad Digital Repository (https://doi.org/10.5061/dryad.p2ngf1w77).

Submitted 30 June 2026
Accepted 18 September 2026
Published 30 October 2026
10.1126/sciadv.aek1491

Downloaded from https://www.science.org at Cornell University on October 30, 2026

ScienceAdvances

Elevated CO_2 mitigated warming-enhanced carbon loss from northern peatland

Jian Zhou, Quan Quan, Wenjuan Huang, Paul J. Hanson, Daniel Ricciuto, Melanie A. Mayes, Natalie A. Griffiths, Verity G. Salmon, Sören Eliot Weber, Jeffrey M. Warren, Richard J. Norby, Mara Y. McPartland, Mirindi Eric Dusenge, Danielle Way, Lifen Jiang, Yu Zhou, Haodi Xu, Feng Tao, Xiaoying Shi, Weinan Chen, Yahai Zhang, and Yiqi Luo

Sci. Adv. **12** (44), eaek1491. DOI: 10.1126/sciadv.aek1491

View the article online
https://www.science.org/doi/10.1126/sciadv.aek1491
Permissions
https://www.science.org/help/reprints-and-permissions

Downloaded from https://www.science.org at Cornell University on October 30, 2026

Use of this article is subject to the Terms of service

Science Advances (ISSN 2375-2548) is published by the American Association for the Advancement of Science. 1200 New York Avenue NW, Washington, DC 20005. The title *Science Advances* is a registered trademark of AAAS.

Copyright © 2026 The Authors, some rights reserved; exclusive licensee American Association for the Advancement of Science. No claim to original U.S. Government Works. Distributed under a Creative Commons Attribution NonCommercial License 4.0 (CC BY-NC).